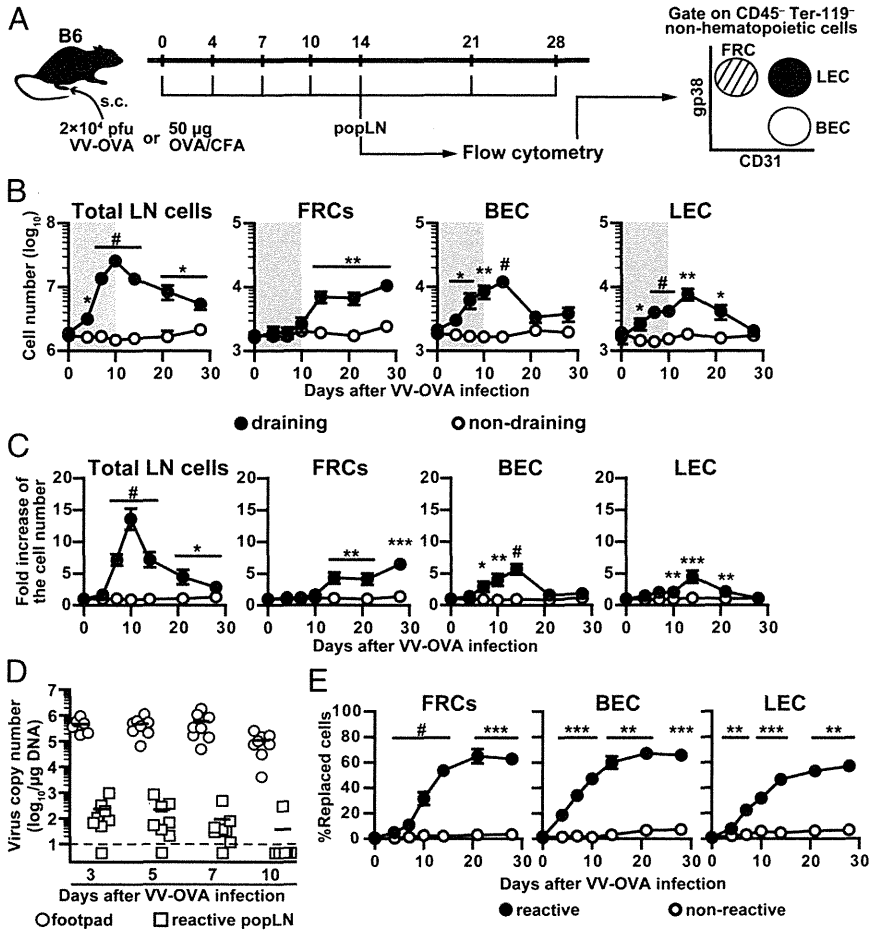

FIGURE 1. Kinetics of the FRC response following immune stimulation. (**A**) Experimental model. On day 0, mice were injected s.c. with VV-OVA or OVA/CFA via the footpad or hock, respectively. LNSC subsets in the reactive and contralateral nonreactive popLNs were analyzed by flow cytometry at various time points. Number (**B**) and fold expansion (**C**) of total LN cells, FRCs, BECs, and LECs in the reactive LNs on days 0, 4, 7, 10, 14, 21, and 28 after VV-OVA infection. Fold expansion for each subset was calculated by normalizing against mean cell number in unstimulated (day 0) popLNs. Shading in (B) indicates the time points across which FRC expansion is delayed. Graphs show the mean ± SEM of $n = 17$/time point, pooled from five independent experiments. (**D**) Kinetics of viral load in the infected footpads (○) and reactive popLNs (□), measured by copy number assay for the *Ova* gene. Each symbol represents one mouse ($n = 8$ pooled from two independent experiments), and horizontal lines indicate means. Dashed line represents the limit of detection. (**E**) Turnover of FRCs, BECs, and LECs was measured by long-term BrdU-labeling assay. Mice were provided with drinking water containing BrdU from day 0 until the time of analysis. Data represent mean ± SEM ($n = 12$/time point) of the proportion of $BrdU^+$ cells in reactive (filled) and contralateral nonreactive (blank) popLNs. Data are pooled from three independent experiments. $^*p < 0.05$, $^{**}p < 0.05$, $^{***}p < 0.001$, $^{\#}p < 0.0001$ versus nonreactive popLNs, Student t test.

We next investigated the turnover of LNSC subsets by continuous BrdU labeling throughout VV-OVA infection (up to day 28 p.i.). In this experimental setting, BrdU incorporation identifies cells that have been replaced within the time frame of the experiment. Turnover of endothelial cells commenced as early as day 4 p.i., whereas there was a marked increase in $BrdU^+$ FRCs from day 7 p.i. (Fig. 1E, Supplemental Fig. 1D). The proportion of $BrdU^+$ cells across all LNSC subsets remained constant after day 14 p.i., suggesting an accelerated turnover rate of these cells during the first 2 wk of acute viral infection. In nonreactive LNs, only minimal turnover of LNSCs was observed across the 28-d duration of our experiments (Fig. 1E).

Immunofluorescent staining of popLN sections revealed that FRCs were present in the central and perivascular areas of the T cell region and the medulla (Fig. 2A). FRC localization was not affected by infection. $BrdU^+$ FRCs (cells that had been replaced p.i.) were found throughout the T cell region after continuous BrdU labeling for 14 d (Fig. 2B). However, the density of $BrdU^+$ FRCs was substantially higher in the perivascular areas of both the T cell region and the medulla (Fig. 2C), suggesting that FRC precursors may be enriched in this subcompartment. Similar results were observed in mice immunized with OVA protein emulsified in CFA (data not shown).

FRCs are terminally differentiated cells that are replenished by local precursors

LNSC turnover could result from two possible events: proliferation of LNSCs themselves and/or differentiation from stromal precursor cells. We evaluated the proliferation of LNSCs after viral infection using short-term in vivo BrdU pulse-labeling experiments (Fig. 3A). Although BrdU incorporation by BECs and LECs was evident as early as day 3 p.i. and was detectable until day 14, minimal FRC proliferation was detected in reactive popLNs and only on day 7 p.i. (Fig. 3B). The low proliferation of FRCs was confirmed using #639/#474 mice, which were engineered to allow visualization of cell cycle progression in a labeling-free manner through the reciprocal expression of Cdt1-coupled Kusabira-Orange and geminin-coupled Azami-Green during the G_1 and $S/G_2/M$ phases of the cell cycle, respectively (18) (Fig. 3C). Taken together, our data suggest that FRC expansion is initiated by the generation of new FRCs by intranodal precursor cells, rather than the proliferation of terminally differentiated mature FRCs. Of note, the expansion and turnover of total $CD45^-$ $CD31^-$ $gp38^-$ double negative (DN) cells progressed with similar kinetics to those of FRCs (Supplemental Fig. 2A, 2B). Moreover, there was a readily detectable proportion of proliferating cells within the $LT\beta R^+$ $CD31^-$ $gp38^-$ DN LNSC population in reactive PLNs (Supplemental Fig. 2C), which could contain FRC precursor cells (11).

We also addressed whether FRCs might be replenished by circulating progenitors recruited to reactive LNs after viral infection. However, parabiosis experiments suggested that newly generated FRCs were likely derived from intranodal cells. Reactive popLNs in wild-type (WT) parabionts conjoined with type I collagen α2 (Col1a2) GFP reporter mice (19) did not contain GFP-expressing FRCs on day 14 p.i. (Supplemental Fig. 2D), when FRC turnover reached a plateau (Fig. 1E). The presence of GFP^- FRCs in the reactive popLNs is consistent with a previous report

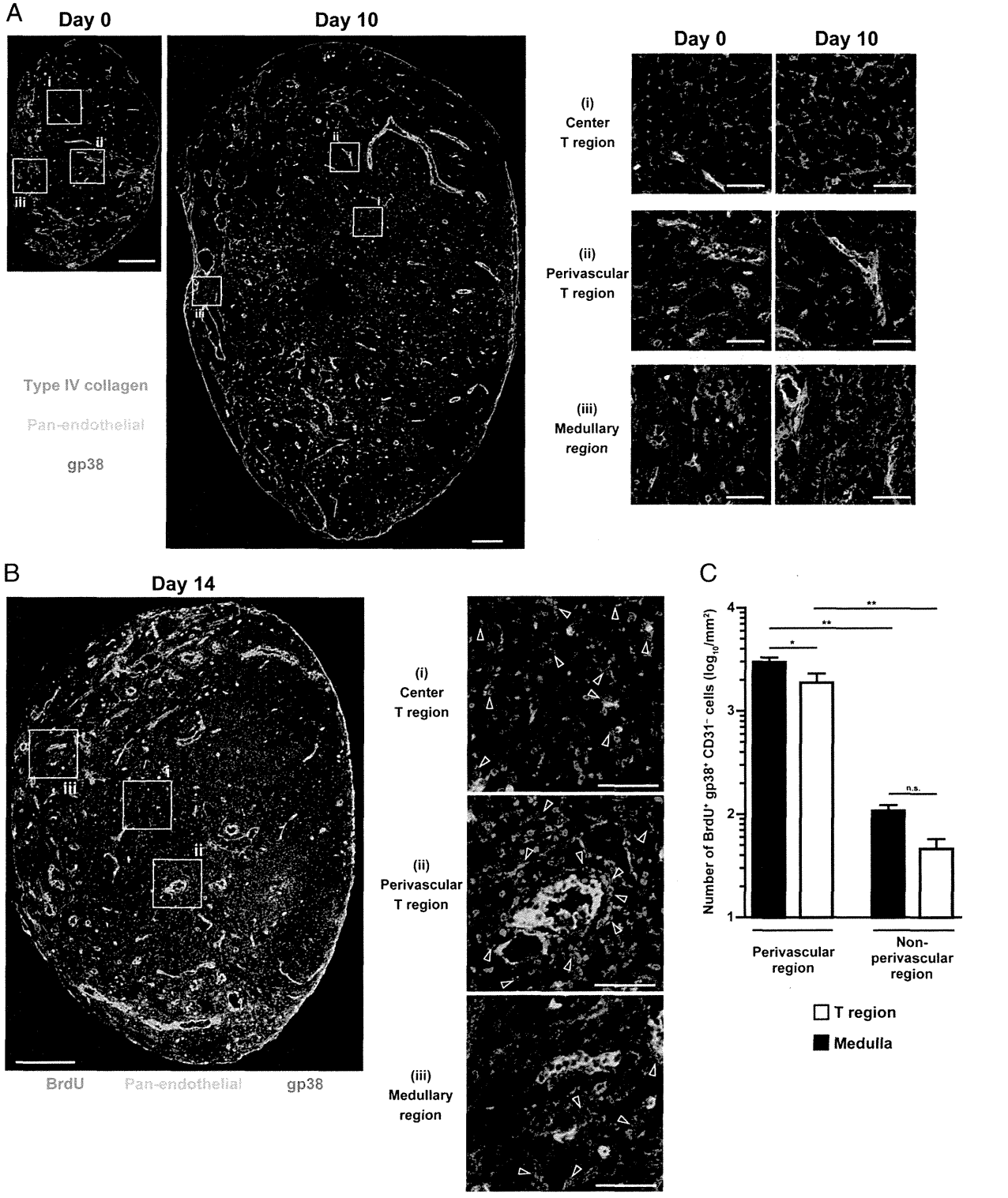

FIGURE 2. Localization of FRCs following s.c. VV-OVA infection. (**A**) Localization of FRCs in the reactive popLNs on days 0 and 10 p.i. Red, type IV collagen; green, pan-endothelial Ag; blue, gp38. Enlarged views of specific areas in the LN (*right panels*): (**i**) center of T cell region, (**ii**) perivascular area in the T cell region, and (**iii**) medulla. (**B**) Localization of $BrdU^+$ FRCs in the reactive popLNs on day 14 p.i. BrdU labeling was performed as for Fig. 1E. Enlarged views show specific areas as in (A), depicted as (**i**), (**ii**), and (**iii**). Red, BrdU; green, pan-endothelial Ag; blue, gp38. Arrowheads indicate $BrdU^+$ FRCs. Scale bars, 200 μm (*left panels*) and 50 μm (*right panels*). Representative images from six LNs are shown. (**C**) Number of $BrdU^+$ $gp38^+$ cells/mm^2 of different regions of the reactive popLNs on day 14 p.i. Three sections/LN that were ≥50 μm from each other were used for quantification. Graph shows mean ± SEM of $n = 6$ pooled from two independent experiments. $^*p < 0.05$, $^{**}p < 0.001$, one-way ANOVA with Bonferroni post hoc test. n.s., not significant.

using these reporter mice that showed that phenotypic fibroblasts in the CCl_4-treated liver also contain a GFP^- population (19). This could be due either to transcription of *Col1a2* by only a limited fraction of FRCs in a manner independent of the promoter/enhancer used in this transgenic mouse strain or to occasional epigenetic inactivation of the transgene in some FRCs.

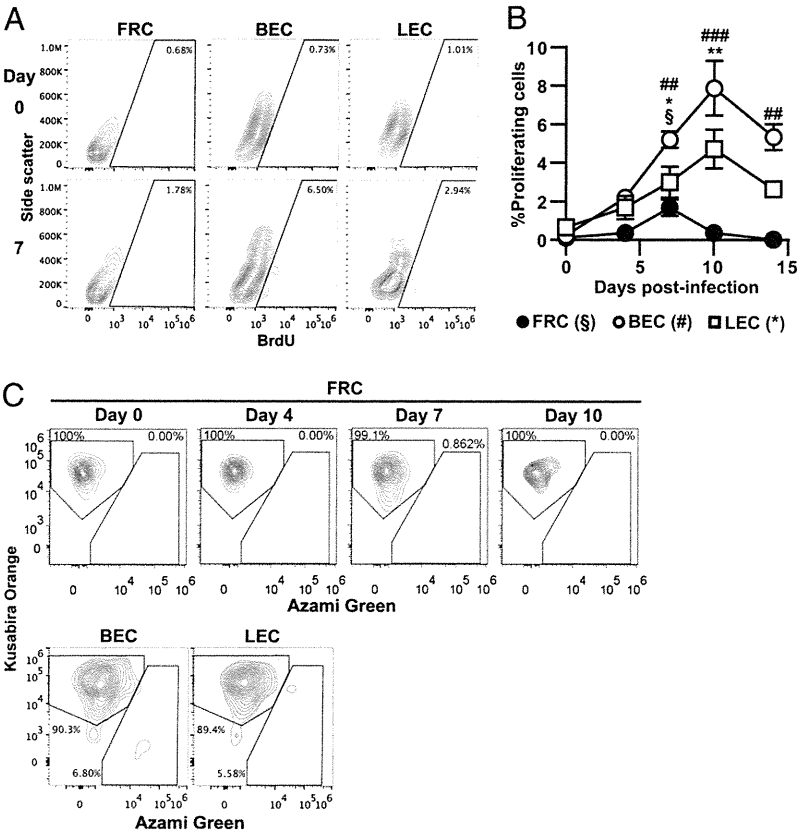

FIGURE 3. Proliferation of FRCs after viral infection. (**A** and **B**) Assessment of LNSC proliferation by short-term BrdU-labeling assay. Proliferating cells were marked by 16-h BrdU pulse labeling. Representative plots on days 0 and 7 (A) and mean ± SEM (B) of n = 12/time point pooled from three independent experiments. $^{*}p < 0.05$, $^{**,\#\#}p < 0.005$, $^{\S,***,\#\#\#}p < 0.0001$, versus day 0, one-way ANOVA with Dunnett post hoc test. The different symbols represent different comparisons as indicated below (B). (**C**) Proliferation of FRCs measured using Fucci transgenic mice. Proliferating cells were identified as Azami-Green–expressing cells. Plots gated on BECs and LECs on day 10 p.i. are shown as a positive control for Fucci-based monitoring of stromal cell proliferation. Representative plots from n = 9 pooled from three independent experiments are shown.

Lymphotoxin signaling regulates sustained LNSC subset expansion

Because LTβR plays an important role in the remodeling and maintenance of function of LNs (11, 24), we examined the involvement of LTβR-mediated signaling in FRC turnover by using the inhibitor LTβR-Ig. Unexpectedly, LTβR-Ig treatment from the time of infection reduced the number of FRCs and total LN cells in reactive popLNs only after day 14 p.i. (Fig. 4A), although FRC turnover was reduced to ~50% of that observed in control mice (Fig. 4B). Similarly, BEC, but not LEC, expansion was severely attenuated by LTβR-Ig treatment only after day 10 p.i. (Fig. 4). Notably, turnover of both FRCs and BECs ceased at earlier time points in LTβR-Ig–treated mice than in control mice. These results suggest that LTβR-mediated signaling contributes to sustained LNSC turnover but that alternative growth pathways play a more important role in the early expansion of LNSCs.

Sustained upregulation of MHC class II on LNSCs

Next, we determined whether FRCs change their activation status during viral infection. Based on flow cytometric analysis, FRCs underwent a progressive increase in cell size (forward scatter) and internal complexity (side scatter) after viral infection (Fig. 5A), indicating that FRCs remained activated from at least day 4 to day 10. β1 integrin, VCAM, CD44, platelet-derived growth factor receptors, CD80, and MHC class I were all expressed constitutively on FRCs (Fig. 5B). MHC class II surface expression levels were elevated on day 10 p.i. (Fig. 5C). Notably, the highest MHC class II expression among LNSCs was detected on CD157^{+} FRCs (Fig. 5D, 5E). This increase was observed in both BrdU^{-} and BrdU^{+} cells in long-term BrdU-incorporation experiments (data not shown).

MHC class II on LNSCs induces CD4^{+} T cell contraction after peak expansion

Based on the increased MHC class II expression detected on LNSCs, we examined the impact of stromal cell–mediated Ag presentation on CD4^{+} T cell responses, with a particular focus on the later time points of the immune response. For this purpose, lethally irradiated CD45.1^{-} CD45.2^{+} WT B6 or mutant *H2-Ab* allele–harboring bm12 mice received adoptive transfer of CD45.1^{+} CD45.2^{+} B6 BM, giving rise to B6→B6 and B6→bm12 chimera, respectively. Chimeric mice received 2 × 10^{4} H2-A^{b}–restricted CD45.1^{+} CD45.2^{-} OT-II T cells, such that the responses of monoclonal T cells with the same TCR and genetic background could be used as a functional readout. Leukocytes from different sources were discriminated using CD45 congenic markers (Fig. 6A). Remnants of recipient leukocytes accounted for 16.1 ± 1.42% and 20.2 ± 1.12% of total leukocytes in the LNs of B6→B6 and B6→bm12 chimeras, respectively. More than 90% of host-derived leukocytes were T cells (data not shown). Importantly, only 0.4 ± 0.1% and 1.3 ± 0.5% of MHC class II^{+} B cells and DCs, respectively, were of recipient origin in the LNs of B6→bm12 mice. Thus, Ag presentation to OT-II T cells in the LNs should occur under comparable conditions in both chimeras, except that LNSCs cannot present cognate peptide to OT-II cells in B6→bm12 mice because of the mutation in the *H2-Ab* gene.

Although OVA infection induced <50-fold expansion of adoptively transferred OT-II CD4^{+} T cells (data not shown), OVA/CFA immunization promoted an ~1000-fold OT-II T cell expansion in both chimeras that peaked by day 10 (Fig. 6B). Of note, we detected a substantially higher number of OT-II T cells in the reactive popLNs of B6→bm12 mice from day 21 onward (Fig. 6B), suggesting that loss of stromal cell–mediated Ag presentation leads to slower contraction of OT-II cells. In line with this observation, the number of OT-II–derived CXCR5^{+} PD-1^{hi} ICOS^{+} T follicular helper (Tfh) cells (25) was increased in B6→bm12 mice on day 21, but not day 10 (Fig. 6C), without any skewing toward Tfh cells (percentage of Tfh cells in total OT-II cells on day 21 was 18.0 ± 5.1% in WT mice and 20.9 ± 3.3% in mutant chimera, p = 0.657, Student t test). Our results demonstrate

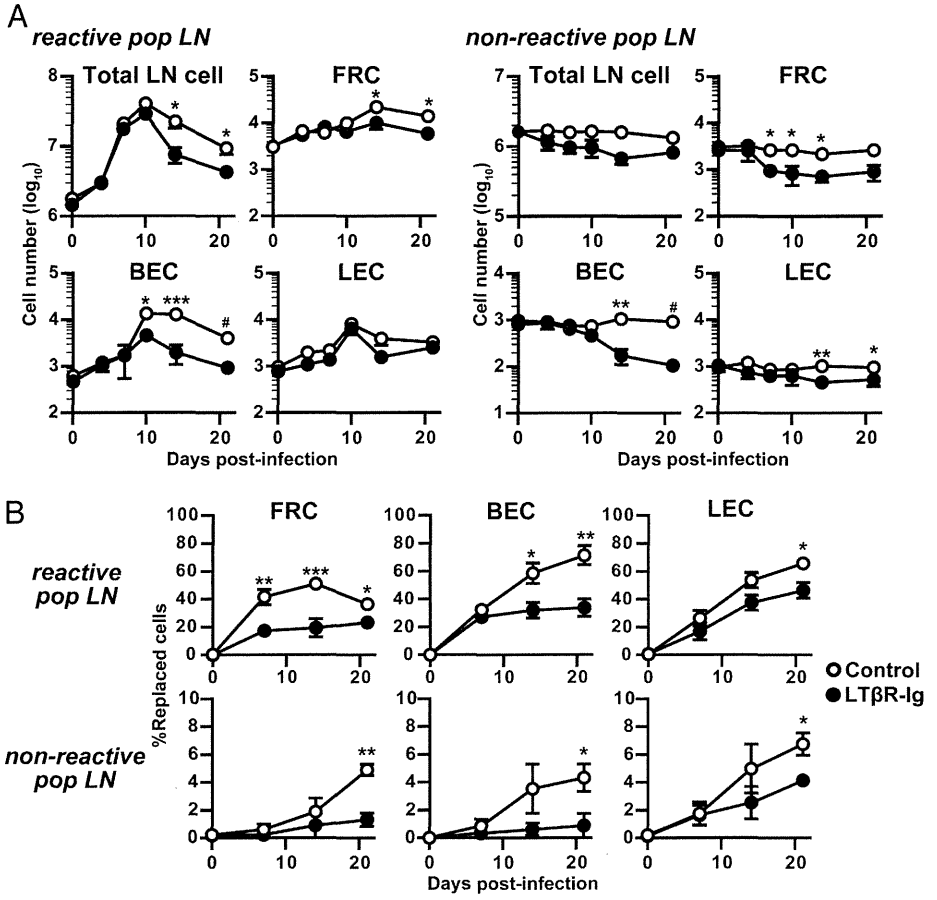

FIGURE 4. Paucity of the BEC and FRC response in the absence of LTβR-mediated signaling. Mice were injected i.p. with 100 μg LTβR-Ig once a week starting from the day before immunization. The number (**A**) and turnover (**B**) of FRCs, BECs, and LECs after VV-OVA infection were measured by flow cytometry. The results of statistical analyses comparing cell numbers against the initial number on day 0 by one-way ANOVA are summarized in Supplemental Table I. Turnover was assessed as for Fig. 1D by performing long-term BrdU-labeling assays. Graphs show the mean ± SEM of $n = 9$/time point pooled from three independent experiments. $^{*}p < 0.05$, $^{**}p < 0.01$, $^{***}p < 0.005$, $^{\#}p < 0.001$, reactive versus nonreactive popLNs, unpaired Student t test.

that Ag presentation by stromal cells negatively modulates the later phase of the Ag-specific $CD4^+$ T cell response.

Discussion

Although LNSCs are now recognized to play an important role in the adaptive immune response, the dynamic changes that occur in the number and function of these cells during physiologically relevant virus infection have not been investigated previously. In the current study, we used a cytopathic virus to monitor the growth and differentiation of LNSCs, with a focus on FRCs. We report a delayed, but sustained, expansion of FRCs, which was not synchronized with the expansion of other LNSC subsets or total LN cell numbers. Our data support a model in which FRCs are replenished in an LTβR-dependent manner by local precursors accumulated in the perivascular areas. At the peak of the adaptive immune response, LNSC subsets increase MHC class II expression, which contributes to $CD4^+$ T cell contraction.

Contrary to our expectation that all LNSCs would expand in parallel with incoming leukocyte numbers following viral infection, we observed substantially delayed growth of FRCs during the first week of infection. In immunofluorescent sections of reactive LNs, the FRC network on day 10 p.i. appeared more sparse compared with FRCs in control LNs. This observation may indicate the formation of a more widely spaced stromal network, either owing to mechanical stretching to accommodate increased leukocyte numbers or as a result of the death of FRCs in infected LNs. In contrast, Luther and colleagues (26) reported comparable spacing of the FRC network after immunization with a protein Ag emulsified in an adjuvant. This discrepancy may be the result of the different kinetics of FRC expansion between sterile inflammation and our viral infection models. Two weeks after viral infection, ~60% of FRCs had been replaced without substantial cellular proliferation of mature FRCs. BrdU-incorporating cells among the perivascular DN LNSC population (11) may generate new FRCs during viral infections, which is consistent with the dense accumulation of $BrdU^+$ FRCs around blood vessels that was observed in our long-term BrdU-labeling assay. The observation that increased FRC generation depends on LTβR is in line with a recent report by Ludewig and colleagues (11) showing that *Ccl19* promoter–driven conditional ablation of LTβR eliminates mature FRCs but increases the fraction of DN LNSCs. An attractive hypothesis is that high levels of lymphotoxin expression by activated lymphocytes (27) triggers the differentiation of FRCs through direct interaction with intranodal FRC precursor cells. In addition, lymphotoxin signaling may also indirectly affect FRC turnover, because LTβR blockade severely attenuated BEC expansion in LTβR-Ig–treated mice. It is noteworthy that LTβR plays an important role in remodeling (28–30) and in the functional maintenance (24) of high endothelial venules (HEVs). Long-term LTβR-Ig treatment causes a loss of HEV phenotype (24), resulting in the impaired recruitment of lymphocytes into reactive LNs during the ongoing immune response. Because our experiments extended until day 21 p.i., it is likely that HEV function was also impaired in our experiments, which, together with the attenuated BEC response, might result in the suboptimal functional adaptation of LNSCs. A potential mechanism for the attenuated LNSC response in LTβR-Ig treatment could involve, but is not limited to, a decreased amount of unidentified factors provided from recruited lymphocytes and/or BECs. In contrast, the FRC response may facilitate the BEC response, as was suggested by recent studies (13, 22), thus establishing a positive-feedback loop. Taken together, our data support a model in which FRC precursors are

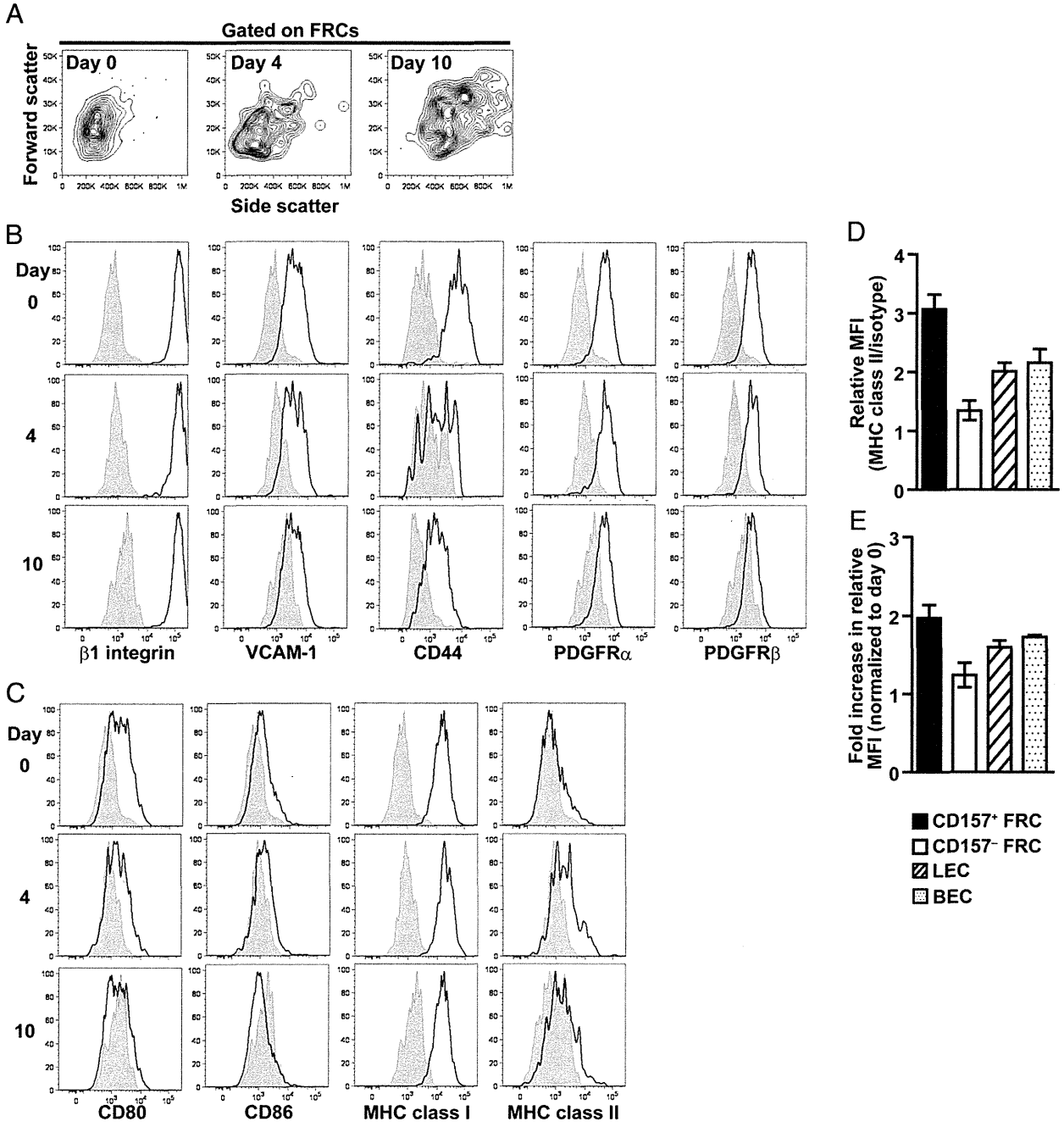

FIGURE 5. Functional changes in FRCs during viral infection. Scatter profile (**A**) and the expression of cell surface markers and MHCs (**B** and **C**) on FRCs in reactive popLNs after VV-OVA infection was analyzed by flow cytometry on days 0 (naive), 4, and 10 p.i. (**D**) Relative mean fluorescent intensity (MFI) values for MHC class II staining on day 10 p.i. Relative MFI was calculated by normalizing absolute MHC class II MFI values against MFI values for isotype-matched control staining of the same sample, to account for variations in the background intensity of each subset. (**E**) Fold increase in relative MFI of MHC class II on day 10 p.i. Representative plots (A–C) and the mean ± SEM (D and E) of $n = 9$ pooled from three independent experiments are shown.

dormant in perivascular niches. In reactive LNs, the increased influx of T and B cells, as well as other leukocytes, triggers LTβR-dependent proliferation and the gradual differentiation of the precursors into mature, nondividing FRCs. Our data also illustrate the flexibility of the adaptive immune response. Although LNSCs undergo steady growth largely parallel to leukocyte influx during sterile inflammation, cytopathic VV infections result in delayed FRC growth. However, the lymphocyte influx that is important for clonal selection is not impaired. In future studies, it will be interesting to analyze how the migratory behavior of lymphocytes changes in cytopathic VV infections.

The increased MHC class II expression by LNSCs that persisted for a long time p.i. suggests that the timing and extent of Ag presentation by LNSCs and the inflammatory microenvironment that supports Ag presentation influence the outcome of stromal Ag presentation. Possible outcomes are the maintenance of self-tolerance (31, 32), the induction of proliferation (16), or the culling of late T cell responses. In terms of the timing of Ag presentation, stromal cells in nonlymphoid tissues could also contribute to late Ag presentation to activated/effector CD4+ T cells in our BM chimera model. Although we cannot exclude this possibility, it is noteworthy that, in our experiments, total and Tfh OT-II cells were similarly

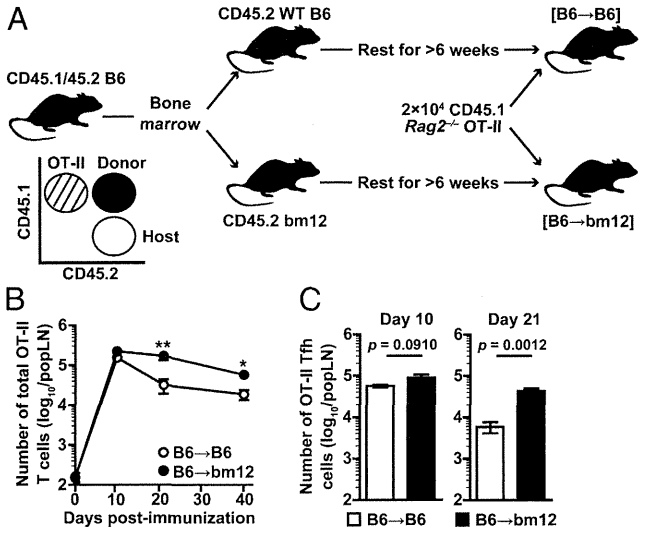

FIGURE 6. Direct Ag presentation by LNSCs curtails the CD4$^+$ T cell response. (**A**) Experimental model. Lethally irradiated CD45.1$^-$ CD45.2$^+$ WT B6 or bm12 recipient mice received 5×10^6 BM cells from CD45.1$^+$ CD45.2$^+$ B6 mice. More than 6 wk later, chimeric mice received 2×10^4 CD45.1$^+$ CD45.2$^-$ *Rag2*$^{-/-}$ OT-II cells and were immunized with OVA/CFA via the hind hock. Donor, recipient, and transgenic T cells were identified by their expression of congenic markers. (**B**) Number of total OT-II T cells in B6 (○) and bm12 (●) recipients after immunization. $*p = 0.0177$, $**p = 0.003$. (**C**) Number of OT-II T cells differentiated into CXCR5^{hi} ICOS$^+$ PD-1^{hi} Tfh cells. Statistical significance was assessed by unpaired Student *t* test. Graphs show the mean ± SEM of $n = 7$–9/time point pooled from three independent experiments.

affected by the loss of Ag presentation by stromal cells. Compared with other effector CD4$^+$ T cells, Tfh cells are long-term LN residents (33, 34) and, therefore, are less likely to encounter stromal cells in nonlymphoid tissues. Accordingly, the decreased number of Tfh cells in the absence of Ag presentation by stromal cells is likely due to the lack of Ag presentation by LNSCs. It would be worthwhile for future studies to analyze the significance of Ag presentation by stromal cells in nonlymphoid tissues, particularly in the context of tissue-resident memory T cell generation.

In conclusion, we provide novel insights into the diverse nature of LNSC responses during viral infection. We propose that LNSCs serve as an extrinsic "brake system" for late CD4$^+$ T cell responses, preventing overt responses after Ag clearance. This idea is supported, at least in part, by recent findings that the potential loss of functional FRCs in chronically SIV-infected macaques coincides with the accumulation of Tfh cells (35–37). Altered FRC functionality is also observed as decreased CCR7 ligand levels and smaller T cell regions in lupus-prone mice, which may relate to impaired immunoregulatory function (38). Furthermore, disruption of functional LN structure in graft-versus-host disease patients (39) likely involves the loss of LNSC function, which may contribute to the autoimmune-like chronic symptoms observed in this disease (40). Further studies in these different contexts will uncover the significance of this putative LNSC-mediated brake system and may lead to improved vaccination strategies or therapies for the induction of immunological tolerance.

Acknowledgments

We thank Philippa Marrack for providing VV-OVA, Atsushi Miyawaki for providing #639/#474 mice, Hiroshi Kiyono for the LTβR-Ig expression vector, Hiroyuki Yamamoto for insightful comments on the manuscript, Francis H.W. Shand for scientific editing of the manuscript, and Mizuha Kosugi-Kanaya, Ryu Takahashi, Chiaki Kasahara, Shun-ichi Fujita, Shin Aoki, Fumika Nakamura, and Ai Yamashita for excellent technical support.

Disclosures

The authors have no financial conflicts of interest.

References

1. Tomura, M., N. Yoshida, J. Tanaka, S. Karasawa, Y. Miwa, A. Miyawaki, and O. Kanagawa. 2008. Monitoring cellular movement in vivo with photoconvertible fluorescence protein "Kaede" transgenic mice. *Proc. Natl. Acad. Sci. USA* 105: 10871–10876.
2. Mempel, T. R., S. E. Henrickson, and U. H. Von Andrian. 2004. T-cell priming by dendritic cells in lymph nodes occurs in three distinct phases. *Nature* 427: 154–159.
3. Bajénoff, M., J. G. Egen, L. Y. Koo, J. P. Laugier, F. Brau, N. Glaichenhaus, and R. N. Germain. 2006. Stromal cell networks regulate lymphocyte entry, migration, and territoriality in lymph nodes. *Immunity* 25: 989–1001.
4. Schumann, K., T. Lämmermann, M. Bruckner, D. F. Legler, J. Polleux, J. P. Spatz, G. Schuler, R. Förster, M. B. Lutz, L. Sorokin, and M. Sixt. 2010. Immobilized chemokine fields and soluble chemokine gradients cooperatively shape migration patterns of dendritic cells. *Immunity* 32: 703–713.
5. Siegert, S., and S. A. Luther. 2012. Positive and negative regulation of T cell responses by fibroblastic reticular cells within paracortical regions of lymph nodes. *Front. Immunol.* 3: 285.
6. Lämmermann, T., and M. Sixt. 2008. The microanatomy of T-cell responses. *Immunol. Rev.* 221: 26–43.
7. Hara, T., S. Shitara, K. Imai, H. Miyachi, S. Kitano, H. Yao, S. Tani-ichi, and K. Ikuta. 2012. Identification of IL-7-producing cells in primary and secondary lymphoid organs using IL-7-GFP knock-in mice. *J. Immunol.* 189: 1577–1584.
8. Onder, L., P. Narang, E. Scandella, Q. Chai, M. Iolyeva, K. Hoorweg, C. Halin, E. Richie, P. Kaye, J. Westermann, et al. 2012. IL-7-producing stromal cells are critical for lymph node remodeling. *Blood* 120: 4675–4683.
9. Link, A., T. K. Vogt, S. Favre, M. R. Britschgi, H. Acha-Orbea, B. Hinz, J. G. Cyster, and S. A. Luther. 2007. Fibroblastic reticular cells in lymph nodes regulate the homeostasis of naive T cells. *Nat. Immunol.* 8: 1255–1265.
10. Scandella, E., B. Bolinger, E. Lattmann, S. Miller, S. Favre, D. R. Littman, D. Finke, S. A. Luther, T. Junt, and B. Ludewig. 2008. Restoration of lymphoid organ integrity through the interaction of lymphoid tissue-inducer cells with stroma of the T cell zone. *Nat. Immunol.* 9: 667–675.
11. Chai, Q., L. Onder, E. Scandella, C. Gil-Cruz, C. Perez-Shibayama, J. Cupovic, R. Danuser, T. Sparwasser, S. A. Luther, V. Thiel, et al. 2013. Maturation of lymph node fibroblastic reticular cells from myofibroblastic precursors is critical for antiviral immunity. *Immunity* 38: 1013–1024.
12. Woolf, E., I. Grigorova, A. Sagiv, V. Grabovsky, S. W. Feigelson, Z. Shulman, T. Hartmann, M. Sixt, J. G. Cyster, and R. Alon. 2007. Lymph node chemokines promote sustained T lymphocyte motility without triggering stable integrin adhesiveness in the absence of shear forces. *Nat. Immunol.* 8: 1076–1085.
13. Chyou, S., E. H. Ekland, A. C. Carpenter, T. C. J. Tzeng, S. Tian, M. Michaud, J. A. Madri, and T. T. Lu. 2008. Fibroblast-type reticular stromal cells regulate the lymph node vasculature. *J. Immunol.* 181: 3887–3896.
14. Fletcher, A. L., V. Lukacs-Kornek, E. D. Reynoso, S. E. Pinner, A. Bellemare-Pelletier, M. S. Curry, A. R. Collier, R. L. Boyd, and S. J. Turley. 2010. Lymph node fibroblastic reticular cells directly present peripheral tissue antigen under steady-state and inflammatory conditions. *J. Exp. Med.* 207: 689–697.
15. Cohen, J. N., C. J. Guidi, E. F. Tewalt, H. Qiao, S. J. Rouhani, A. Ruddell, A. G. Farr, K. S. Tung, and V. H. Engelhard. 2010. Lymph node-resident lymphatic endothelial cells mediate peripheral tolerance via Aire-independent direct antigen presentation. *J. Exp. Med.* 207: 681–688.
16. Onder, L., E. Scandella, Q. Chai, S. Firner, C. T. Mayer, T. Sparwasser, V. Thiel, T. Rülicke, and B. Ludewig. 2011. A novel bacterial artificial chromosome-transgenic podoplanin-cre mouse targets lymphoid organ stromal cells in vivo. *Front. Immunol.* 2: 50.
17. Malhotra, D., A. L. Fletcher, J. Astarita, V. Lukacs-Kornek, P. Tayalia, S. F. Gonzalez, K. G. Elpek, S. K. Chang, K. Knoblich, M. E. Hemler, et al.; Immunological Genome Project Consortium. 2012. Transcriptional profiling of stroma from inflamed and resting lymph nodes defines immunological hallmarks. *Nat. Immunol.* 13: 499–510.
18. Tomura, M., A. Sakaue-Sawano, Y. Mori, M. Takase-Utsugi, A. Hata, K. Ohtawa, O. Kanagawa, and A. Miyawaki. 2013. Contrasting quiescent G_0 phase with mitotic cell cycling in the mouse immune system. *PLoS ONE* 8: e73801.
19. Higashiyama, R., T. Moro, S. Nakao, K. Mikami, H. Fukumitsu, Y. Ueda, K. Ikeda, E. Adachi, G. Bou-Gharios, I. Okazaki, et al. 2009. Negligible contribution of bone marrow-derived cells to collagen production during hepatic fibrogenesis in mice. *Gastroenterology* 137: 1459–1466.e1.
20. Restifo, N. P., I. Bacík, K. R. Irvine, J. W. Yewdell, B. J. McCabe, R. W. Anderson, L. C. Eisenlohr, S. A. Rosenberg, and J. R. Bennink. 1995. Antigen processing in vivo and the elicitation of primary CTL responses. *J. Immunol.* 154: 4414–4422.
21. Kamala, T. 2007. Hock immunization: a humane alternative to mouse footpad injections. *J. Immunol. Methods* 328: 204–214.
22. Chyou, S., F. Benahmed, J. Chen, V. Kumar, S. Tian, M. Lipp, and T. T. Lu. 2011. Coordinated regulation of lymph node vascular-stromal growth first by CD11c$^+$ cells and then by T and B cells. *J. Immunol.* 187: 5558–5567.
23. Fletcher, A. L., D. Malhotra, S. E. Acton, V. Lukacs-Kornek, A. Bellemare-Pelletier, M. Curry, M. Armant, and S. J. Turley. 2011. Reproducible isolation of lymph node stromal cells reveals site-dependent differences in fibroblastic reticular cells. *Front. Immunol.* 2: 35.

24. Browning, J. L., N. Allaire, A. Ngam-Ek, E. Notidis, J. Hunt, S. Perrin, and R. A. Fava. 2005. Lymphotoxin-β receptor signaling is required for the homeostatic control of HEV differentiation and function. *Immunity* 23: 539–550.
25. Crotty, S. 2011. Follicular helper CD4 T cells (TFH). *Annu. Rev. Immunol.* 29: 621–663.
26. Yang, C. Y., T. K. Vogt, S. Favre, L. Scarpellino, H. Y. Huang, F. Tacchini-Cottier, and S. A. Luther. 2014. Trapping of naive lymphocytes triggers rapid growth and remodeling of the fibroblast network in reactive murine lymph nodes. *Proc. Natl. Acad. Sci. USA* 111: E109–E118.
27. Browning, J. L., I. D. Sizing, P. Lawton, P. R. Bourdon, P. D. Rennert, G. R. Majeau, C. M. Ambrose, C. Hession, K. Miatkowski, D. A. Griffiths, et al. 1997. Characterization of lymphotoxin-α β complexes on the surface of mouse lymphocytes. *J. Immunol.* 159: 3288–3298.
28. Webster, B., E. H. Ekland, L. M. Agle, S. Chyou, R. Ruggieri, and T. T. Lu. 2006. Regulation of lymph node vascular growth by dendritic cells. *J. Exp. Med.* 203: 1903–1913.
29. Kumar, V., E. Scandella, R. Danuser, L. Onder, M. Nitschké, Y. Fukui, C. Halin, B. Ludewig, and J. V. Stein. 2010. Global lymphoid tissue remodeling during a viral infection is orchestrated by a B cell-lymphotoxin-dependent pathway. *Blood* 115: 4725–4733.
30. Kumar, V., S. Chyou, J. V. Stein, and T. T. Lu. 2012. Optical projection tomography reveals dynamics of HEV growth after immunization with protein plus CFA and features shared with HEVs in acute autoinflammatory lymphadenopathy. *Front. Immunol.* 3: 282.
31. Lukacs-Kornek, V., and S. J. Turley. 2011. Self-antigen presentation by dendritic cells and lymphoid stroma and its implications for autoimmunity. *Curr. Opin. Immunol.* 23: 138–145.
32. Fletcher, A. L., D. Malhotra, and S. J. Turley. 2011. Lymph node stroma broaden the peripheral tolerance paradigm. *Trends Immunol.* 32: 12–18.
33. Fazilleau, N., M. D. Eisenbraun, L. Malherbe, J. N. Ebright, R. R. Pogue-Caley, L. J. McHeyzer-Williams, and M. G. McHeyzer-Williams. 2007. Lymphoid reservoirs of antigen-specific memory T helper cells. *Nat. Immunol.* 8: 753–761.
34. Fazilleau, N., L. J. McHeyzer-Williams, H. Rosen, and M. G. McHeyzer-Williams. 2009. The function of follicular helper T cells is regulated by the strength of T cell antigen receptor binding. *Nat. Immunol.* 10: 375–384.
35. Zeng, M., A. J. Smith, S. W. Wietgrefe, P. J. Southern, T. W. Schacker, C. S. Reilly, J. D. Estes, G. F. Burton, G. Silvestri, J. D. Lifson, et al. 2011. Cumulative mechanisms of lymphoid tissue fibrosis and T cell depletion in HIV-1 and SIV infections. *J. Clin. Invest.* 121: 998–1008.
36. Petrovas, C., T. Yamamoto, M. Y. Gerner, K. L. Boswell, K. Wloka, E. C. Smith, D. R. Ambrozak, N. G. Sandler, K. J. Timmer, X. Sun, et al. 2012. CD4 T follicular helper cell dynamics during SIV infection. *J. Clin. Invest.* 122: 3281–3294.
37. Lindqvist, M., J. van Lunzen, D. Z. Soghoian, B. D. Kuhl, S. Ranasinghe, G. Kranias, M. D. Flanders, S. Cutler, N. Yudanin, M. I. Muller, et al. 2012. Expansion of HIV-specific T follicular helper cells in chronic HIV infection. *J. Clin. Invest.* 122: 3271–3280.
38. Abe, J., S. Ueha, J. Suzuki, Y. Tokano, K. Matsushima, and S. Ishikawa. 2008. Increased Foxp3(+) CD4(+) regulatory T cells with intact suppressive activity but altered cellular localization in murine lupus. *Am. J. Pathol.* 173: 1682–1692.
39. Horny, H. P., H. A. Horst, G. Ehninger, and E. Kaiserling. 1988. Lymph node morphology after allogeneic bone marrow transplantation for chronic myeloid leukemia: a histological and immunohistological study focusing on the phenotype of the recovering lymphoid cells. *Blut* 57: 31–40.
40. Tyndall, A., and F. Dazzi. 2008. Chronic GVHD as an autoimmune disease. *Best Pract. Res. Clin. Haematol.* 21: 281–289.

supplemental Table 1 Statistical analysis of Fig.4 cell counts as compared to day 0

Group	Days p.i.	Reactive popLNs				Non-reactive popLNs			
		Total	FRC	BEC	LEC	Total	FRC	BEC	LEC
Control	4	n.s.	n.s.	n.s.	n.s.	n.s.	n.s.	n.s.	n.s.
	7	< 0.001	n.s.	n.s.	n.s.	n.s.	n.s.	n.s.	n.s.
	10	< 0.001	n.s.	< 0.001	< 0.001	n.s.	n.s.	n.s.	n.s.
	14	< 0.001	< 0.001	< 0.001	n.s.	n.s.	n.s.	n.s.	n.s.
	21	n.s.	< 0.005	n.s.	n.s.	n.s.	n.s.	n.s.	n.s.
LTβR-Ig	4	n.s.	n.s.	n.s.	n.s.	n.s.	n.s.	n.s.	n.s.
	7	< 0.001	< 0.05	n.s.	n.s.	n.s.	n.s.	n.s.	n.s.
	10	< 0.001	< 0.05	< 0.005	< 0.001	n.s.	< 0.05	n.s.	n.s.
	14	< 0.05	< 0.005	n.s.	n.s.	< 0.05	< 0.05	< 0.05	n.s.
	21	n.s.	n.s.	n.s.	n.s.	< 0.05	< 0.05	< 0.001	n.s.

Cell numbers at each time point were compared with those on day 0 by one-way ANOVA with Dunnett's post-hoc test.

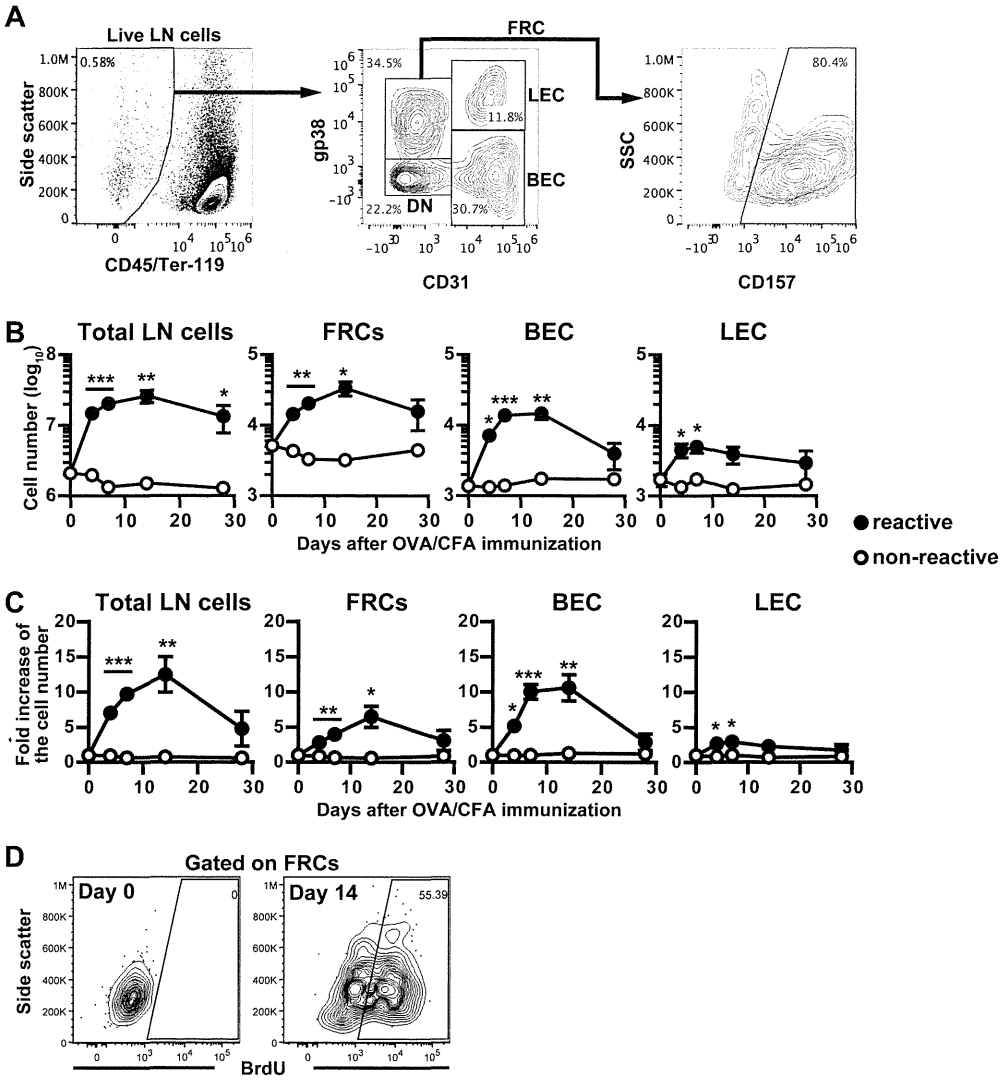

Supplemental Figure 1. Kinetics of LNSC response after OVA/CFA immunization. (A) Gating scheme for the identification of LNSC subsets. Plots from a naive popLN are shown. (B–C) Kinetics of the number (B) and fold-increase (C) of total LN cells, FRCs, BECs and LECs in reactive and contralateral non-reactive popLNs after OVA/CFA immunization. Mice were treated and analyzed as shown in Fig.1A, but immunized with OVA/CFA instead of VV-OVA.Number of LNSCs were assessed on day 0, 4, 7, 14, and 28.Graphs show the mean ± SEM of n = 9 per time point pooled from three independent experiments. $^{*}p < 0.05$, $^{**}p < 0.005$, $^{***}p < 0.001$ by Student' s *t*-test. (D) Flow cytometry of BrdU incorporation by FRCs on day 0 and day 14 p.i. by VV-OVA in long-term BrdU labeling experiments. Representative plots of n = 12 for each time point pooled from three independent experiments are shown.

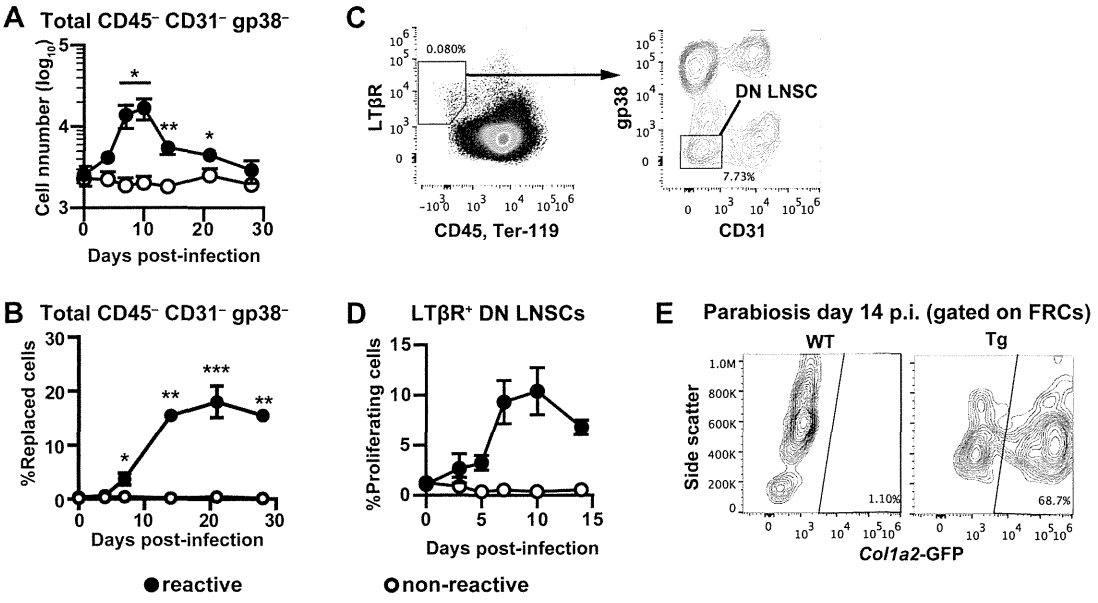

Supplemental Figure 2. Possible contribution of DN LNSCs to FRC turnover. (A) Kinetics of the number of DN cells in reactive popLNs after subcutaneous VV-OVA infection. Graph shows the mean ± SEM of n = 17 per time point pooled from five independent experiments. (B) Turnover of CD45⁻ CD31⁻ gp38⁻ cells in reactive LNs during VV-OVA infection. Graph shows the mean ± SEM of n = 9 per time point pooled from three independent experiments. (C–D) Identification of DN LNSCs (C) and kinetics of the frequency of proliferating LTβR⁺ DN LNSCs (D). Proliferation was measured by 16 hr BrdU pulse labeling. Graph shows the mean ± SEM of n = 7 per time point pooled from two independent experiments. (E) Contribution of blood-borne cells to FRC turnover analyzed by parabiosis between Col1a2-GFP transgenic and wild type mice. Each parabiont was infected with VV-OVA more than 6 weeks after surgery. Prevalence of GFP expressing FRCs in reactive PLNs was monitored by flow cytometry on day 14 post-infection. Note that WT LN is devoid of GFP⁺ cells. Representative data of n = 6 pooled from two independent experiments are shown. *$p < 0.05$, **$p < 0.001$, ***$p < 0.0001$ by Students t-test compared with non-draining popLN.

シンポジウム

3. 臓器の線維化とその治療
1）肝臓の線維化とその治療

稲垣　豊　住吉　秀明

Key words：Liver fibrosis, Fibrogenesis, Fibrolysis, Fibrosis marker

はじめに

肝線維症は，肝炎ウイルスの持続感染やアルコールの過剰摂取，非アルコール性脂肪肝炎(Non-alcoholic steatohepatitis：NASH)の他にも，自己免疫学的機序，肝内胆汁うっ滞，薬剤性，金属代謝異常，うっ血肝など，様々な原因により引き起こされる共通の病態である．線維化進展に伴って，肝組織中にはコラーゲンをはじめとする細胞外マトリックスが過剰に沈着し，その終末像である肝硬変では肝細胞機能不全や門脈圧亢進症が進行する．さらに，高頻度に合併する肝細胞癌の発生を抑止するうえでも，肝線維化機序の解明と治療法の開発は喫緊の研究テーマである．肝線維化の過程における星細胞の活性化機序や，線維組織中に増加するコラーゲンとその分解酵素の産生調節機構など，肝線維化研究は近年大きな進歩を遂げた．

しかしながら，臨床の現場に目を向けると，今もって肝線維症に対する特異的かつ効果的な治療薬は存在しない．培養細胞を用いた試験や動物実験によって多くの抗線維化作用物質が同定・報告されていながら，なぜ臨床で充分な効果を発揮できないのであろうか．本稿では，肝線維症の可逆性や肝線維症治療が従前にも増して重要視されている背景を概説するとともに，新たな治療薬の開発と臨床応用に向けて克服すべき問題と今後の展望について論じたい．

1．肝線維化は可逆的な病態である

肝線維化研究の先達であるPérez-TamayoやRojkindらが臨床例における肝硬変の可逆性を指摘して以来，すでに半世紀近くが経過した．当初はヘモクロマトーシスやWilson病といった代謝性疾患の報告が多かったが，その後のウイルス性肝炎に対する治療法の進歩は，その原因の如何を問わずに肝線維化の改善が起こりうることを証明した．アルコール性肝硬変の禁酒症例

東海大学医学部再生医療科学，東海大学大学院医学研究科マトリックス医学生物学センター

111th Scientific Meeting of the Japanese Society of Internal Medicine:Symposium:3. Fibrosis of the viscera and its treatment; 1）Reversibility and treatment of liver fibrosis.

Yutaka Inagaki and Hideaki Sumiyoshi：Department of Regenerative Medicine, School of Medicine, Tokai University, Japan and Center for Matrix Biology and Medicine, Graduate School of Medicine, Tokai University, Japan.

本講演は，平成26年4月13日（日）東京都・東京国際フォーラムにて行われた．

表. 抗線維化効果が認められた肝疾患治療

疾患名	薬剤名または治療方法	文献
C型慢性肝炎	インターフェロン単独療法	Shiratori Y. *Ann Intern Med* (2000)[1]
C型肝硬変	ペグインターフェロン・リバビリン併用療法	Poynard T. *Gastroenterology* (2002)[2]
B型慢性肝炎	ラミブジン	Dienstag JL. *Gastroenterology* (2003)[3]
	エンテカビル	Chang T-T. *Hepatology* (2010)[4]
自己免疫性肝炎	ステロイド	Dufour JF. *Ann Intern Med* (1997)[5]
	アザチオプリン	
原発性胆汁性肝硬変	ウルソデオキシコール酸	Corpechot C. *Hepatology* (2000)[6]
胆管狭窄型慢性膵炎	内視鏡的ドレナージ	Hammel P. *N Engl J Med* (2001)[7]

など，日常臨床で感じていた肝線維化の可逆性が実証された意義は大きい．

これまでに抗線維化効果が認められた肝疾患治療のうち，主なものを表にまとめた．中でも，C型慢性肝炎に対するインターフェロン単独療法[1]やC型肝硬変に対するペグインターフェロン・リバビリンの併用療法[2]，B型慢性肝炎に対するラミブジン[3]やエンテカビル[4]を用いた抗ウイルス療法など，原因療法が奏功した症例における肝線維化の改善は顕著である．また，自己免疫性肝炎に対する免疫抑制療法[5]，原発性胆汁性肝硬変症（primary biliary cirrhosis）に対するウルソデオキシコール酸治療[6]，胆管狭窄型慢性膵炎に伴う胆汁うっ滞型肝線維症に対する内視鏡的ドレナージ[7]でも，その進展要因を排除することにより線維化改善が認められている．

2. 今，なぜ肝線維化研究が注目されているのか？

これまで遅れていた肝線維化研究と線維症治療薬開発の試みが最近にわかに活発になってきたのには，いくつかの理由がある．まず第一に，ウイルス性慢性肝炎に対する治療法の進歩により，近い将来にはNASHが慢性肝疾患の主因となることが予想されるなど，肝臓病診療には大きなパラダイムシフトが起こっている．NASHに対しても体重の減量以外に特異的治療法が存在しない現在，早期から線維化進展を防ぐ薬剤，あるいは肝硬変症例に対して線維の蓄積を減少させて肝細胞機能の回復や肝発癌の抑止をもたらすような薬剤の登場が熱望されている．すなわち，肝線維症はポスト肝炎ウイルス時代の治療ターゲットと言える．

第二に，上述したように抗ウイルス治療法の進歩は，肝線維症が可逆的な病態であることを証明した．組織におけるコラーゲン含量は，合成と分解とのバランスの上に成り立っており，コラーゲン合成を抑制する，あるいは分解を適切に誘導することで，肝線維症は治療可能な病態であることが改めて認識された．

第三に，肝線維症に対する非侵襲的評価方法の開発が挙げられる．これまで検討されてきた血中線維化マーカーに加えて，超音波装置[8]やMR[9]を用いた肝の弾性度診断が可能になった．後述するように，弾性度診断も線維化治療の効果判定には必ずしも十分とは言えないが，肝線維症に対する介入試験を実施する際に，多数の症例の中から比較的均一な対象集団を設定するうえで大きな力となることが期待されている．

最後に，近年の再生医学・再生医療の進歩は，肝線維症の病態研究や治療戦略についても大きな知見をもたらした．肝の線維化と再生とは常に表裏一体の関係にあり，線維化が進行した肝臓では再生が妨げられ，逆に再生状態にある肝臓は線維化刺激の影響を受けにくい．肝線維化と再生の病態連繋に立脚した，新たな線維化治療法が模索されている．

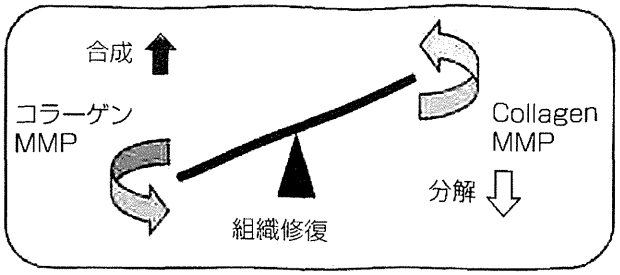

図 1. 臓器線維症におけるマトリックス代謝の変容
組織におけるコラーゲンの含量は，合成と分解のバランスの上に規定されている．その適切な発現は組織修復や創傷治癒過程において重要な働きを演じているが，調節機構が破綻を来たすと組織に過剰のコラーゲンが沈着し，諸臓器の線維化を引き起こす．MMP, matrix metalloproteinase(s)．

3. 肝線維症の治療戦略

前述したように，組織におけるコラーゲン含量は合成と分解とのバランスの上に成り立っており，その均衡が破綻して相対的な合成優位に傾くと，肝をはじめとする諸臓器の線維化を引き起こす（図 1）．端的に言ってしまえば，臓器線維症治療とはマトリックスの合成系と分解系のバランスの是正にほかならない．

肝線維化の進展と改善過程（図 2）から見た治療戦略は，①星細胞活性化の抑制，②活性化星細胞によるコラーゲン産生の抑制，③活性化星細胞に対するアポトーシスないし「脱」活性化の誘導，④Matrix metalloproteinase（MMP）によるコラーゲン線維の分解という各ステップに大別できる．中でも，線維化改善過程における活性化星細胞の脱活性化は注目に値する．肝線維化所見が改善する際には活性化星細胞は急激に減少し，これまではアポトーシスや老化に陥ると考えられてきた．最近になって，活性化した星細胞の約半数が非活性型に戻る（脱活性化）という報告がなされた[10,11]．しかしながら，肝線維化の改善に伴って脱活性化した星細胞は線維化刺激を全く受けていない静止期の星細胞と同一とは言えず，再度の線維化刺激に対する反応性も高いという．星細胞が有するこの可逆性を肝線維症の治療に応用するには，さらに詳細なメカニズムの解明が必要である．

4. 肝線維化治療薬の開発と臨床応用を妨げるものは何か？

肝線維化の進展と改善機序について多くの知見が集積されてきたにもかかわらず，前述した原因治療薬以外には，肝線維症に対する特異的かつ効果的な治療薬はいまだ存在しない．例えばNASHについては，その病態形成にperoxisome proliferator-activated receptor γ（PPAR-γ）シグナルや酸化ストレスの関与が指摘されているにもかかわらず，ピオグリタゾン投与の有効性を示した報告[12]を除くと，グリタゾン製剤やビタミンEの肝線維化抑制効果は概して否定的である[13,14]．また，C型慢性肝炎に対する抗ウイルス療法の非著効例に対して，インターロイキン 10[15]やインターフェロンγ[16]，さらにはグリタゾン製剤[17]の投与が試みられたが，いずれも組織学的には無効であった．また，アンギオテンシンII受容体拮抗薬の投与が肝組織中の酸化ストレスや線維化関連遺伝子の発現を抑制したことで，その抗線維化効果が期待されたが，長期投与では十分な線維化抑制効果は得られなかった[18]．

このように，いわゆる「線維症治療薬」が奏功しない理由としては，薬効自体の限界や副作用の懸念のみならず，臨床研究デザインの限界が挙げられる．すなわち，様々な経過をたどる多くの慢性肝疾患患者の中から比較的均一な対象集団を設定し，通常 10 年単位の長期経過をたどる肝線維症に対する薬物の投与効果を，1 年前後という短期間の介入試験で評価することの困難さがある．肝組織生検は今なお最も信頼できる肝線維症の診断手段であるが，全症例に対し

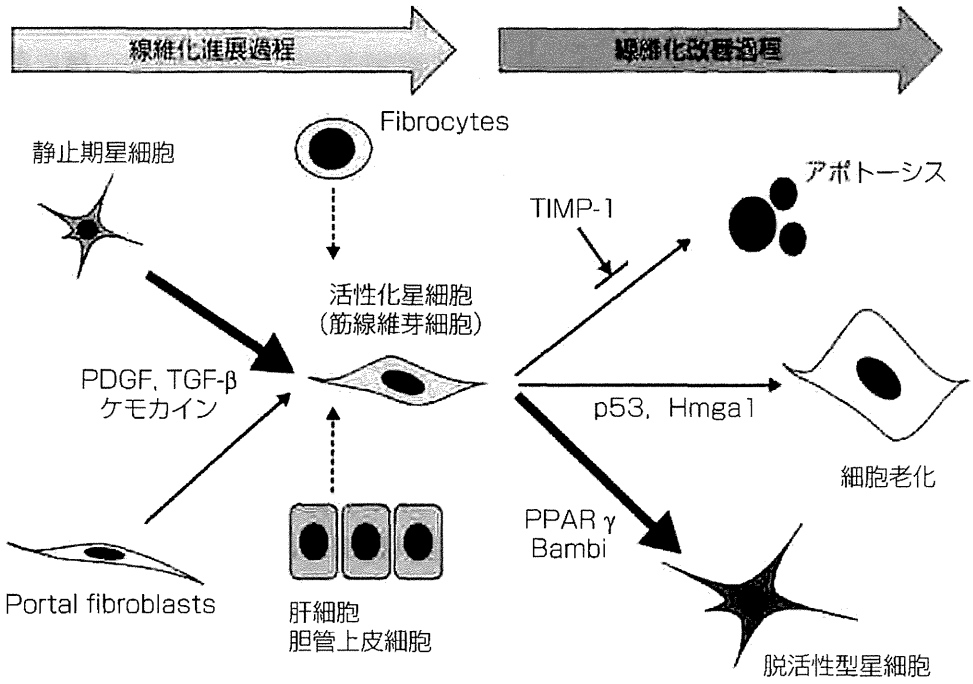

図2. 肝線維化の進展ならびに改善過程

肝実質内の星細胞や門脈域に存在するportal fibroblastsは，肝線維化刺激によって筋線維芽細胞に形質転換して，活発にコラーゲンを産生する．近年では造血細胞由来のFibrocytesや，肝細胞ないし胆管上皮細胞の上皮間葉移行（Epithelial-to-mesenchymal transition, EMT）を介したコラーゲン産生が注目されたが，その後の研究ではその関与は限局的ないし否定的とする意見が多い．一方，肝線維化の改善過程においては，活性化星細胞はアポトーシスや細胞老化に陥ることで排除されると考えられていたが，最近になってその約半数が非活性型に移行（脱活性化）することが報告された．PDGF, platelet-derived growth factor；TGF-β, transforming growth factor-β；TIMP, tissue inhibitor of metalloproteinase, PPARγ, peroxisome proliferator-activated receptor γ.

て治療前後で実施することは現実的でない．また，肝生検のstage分類で得られる線維化情報は組織に沈着したコラーゲン線維の半定量化であり，静的な指標である．近年開発された超音波装置やMRを用いた肝の弾性度診断も，その低侵襲性や定量性には大きな利点があるものの，基本的には組織のコラーゲン蓄積量を反映している．感度および特異度に優れた肝線維化の非侵襲的診断方法，しかも線維症の程度(fibrosis)ではなく，コラーゲンの合成（fibrogenesis）と分解（fibrolysis）の動的な評価系が熱望される所以である．最近，血中タンパク質の糖鎖構造の変化が肝線維化の進展と改善を鋭敏に反映することが報告された[19]．肝線維化の新たな動的マーカーとしての有用性に大きな期待が寄せられている．

おわりに

かつての病理学や肝臓病学の教科書に「肝硬変は進行性かつ不可逆的な疾患である」と記載されていたのは，肝線維症に対する効果的な治療法が存在せず，コラーゲン産生を来たす刺激が慢性的に反復していたからにほかならない．近年の肝線維症治療薬の開発に対する産学の関心の高まりは著しい．肝線維化の可逆性を最大限活かして線維化治療薬の一刻も早い臨床応用に結び付けるには，候補薬剤の開発と並んで，

臨床的に線維化抑制効果の動的評価系の構築が必須であり，さらなる研究と工夫が求められている．

著者のCOI(conflicts of interest)開示：稲垣　豊：研究費・助成金（住友化学）

文　献

1) Shiratori Y, et al : Histological improvement of fibrosis in patients with hepatitis C who have sustained response to interferon therapy. Ann Intern Med 132 : 517–524, 2000.
2) Poynard T, et al : Impact of pegylated interferon alpha-2b and ribavirin on liver fibrosis in patients with chronic hepatitis C. Gastroenterology 122 : 1303–1313, 2002.
3) Dienstag JL, et al : Histological outcome during long-term lamivudine therapy. Gastroenterology 124 : 105–117, 2003.
4) Chang T-T, et al : Long-term entecavir therapy results in the reversal of fibrosis/cirrhosis and continued histological improvement in patients with chronic hepatitis B. Hepatology 52 : 886–893, 2010.
5) Dufour JF, et al : Reversibility of hepatic fibrosis in autoimmune hepatitis. Ann Intern Med 127 : 981–985, 1997.
6) Corpechot C, et al : The effect of ursodeoxycholic acid therapy on liver fibrosis progression in primary biliary cirrhosis. Hepatology 32 : 1196–1199, 2000.
7) Hammel P, et al : Regression of liver fibrosis after biliary drainage in patients with chronic pancreatitis and stenosis of the common bile duct. N Engl J Med 344 : 418–423, 2001.
8) Berzigotti A, et al : Update on ultrasound imaging of liver fibrosis. J Hepatol 58 : 180–182, 2013.
9) Wang Q-B, et al : Performance of magnetic resonance elastography and diffusion-weighted imaging for the staging of hepatic fibrosis : A meta-analysis. Hepatology 56 : 239–247, 2012.
10) Kisseleva T, et al : Myofibroblasts revert to an inactive phenotype during regression of liver fibrosis. Proc Natl Acad Sci USA 109 : 9448–9453, 2012.
11) Troeger JS, et al : Deactivation of hepatic stellate cells during liver fibrosis resolution in mice. Gastroenterology 143 : 1073–1083, 2012.
12) Aithal GP, et al : ndomized placebo-controlled trial of pioglitazone in nondiabetic subjects nonalcoholic steatohepatitis. Gastroenterology 135 : 1176–1184, 2008.
13) Ratziu V, et al : ong-term efficacy of rosiglitazone in nonalcoholic steatohepatitis : results of the fatty liver improvement by rosiglitazone therapy (FLIRT 2) extension trial. Hepatology 51 : 445–453, 2010.
14) Sanyal AJ, et al : ioglitazone, vitamin E, or placebo for nonalcoholic steatohepatitis. N Engl J Med 362 : 1675–1685, 2010.
15) Nelson DR, et al : Long-term interleukin 10 therapy in chronic hepatitis C patients has a proviral and anti-inflammatory effect. Hepatology 38 : 859–868, 2003.
16) Pockros PJ, et al : Final results of a double-blind, placebo-controlled trial of the antifibrotic efficacy of interferon-gamma 1b in chronic hepatitis C patients with advanced fibrosis or cirrhosis. Hepatology 45 : 569–578, 2007.
17) McHutchison J, et al : Farglitazar lacks antifibrotic activity in patients with chronic hepatitis C infection. Gastroenterology 138 : 1365–1373, 2010.
18) Abu Dayyeh BK, et al : The effects of angiotensin blocking agents on the progression of liver fibrosis in the HALT-C Trial cohort. Dig Dis Sci 56 : 564–568, 2011.
19) Kuno A, et al : A serum "sweet-doughnut" protein facilitates fibrosis evaluation and therapy assessment in patients with viral hepatitis. Sci Rep 3 : 1065, 2013. doi : 10.1038/srep01065.

Hepatology Research

Hepatology Research 2015; 45: 29–37 doi: 10.1111/hepr.12349

Review Article

Stem and progenitor cell systems in liver development and regeneration

Akihide Kamiya[1] and Yutaka Inagaki[2]

[1]Laboratory of Stem Cell Therapy, Institute of Innovative Science and Technology, and [2]Department of Regenerative Medicine, Center for Matrix Biology and Medicine, Tokai University School of Medicine, Isehara, Japan

The liver comprises two stem/progenitor cell systems: fetal and adult liver stem/progenitor cells. Fetal hepatic progenitor cells, derived from foregut endoderm, differentiate into mature hepatocytes and cholangiocytes during liver development. Adult hepatic progenitor cells contribute to regeneration after severe and chronic liver injuries. However, the characteristics of these somatic hepatic stem/progenitor cells remain unknown. Culture systems that can be used to analyze these cells were recently established and hepatic stem/progenitor cell-specific surface markers including delta-like 1 homolog (DLK), cluster of differentiation (CD) 13, CD133, and LIV2 were identified. Cells purified using antibodies against these markers proliferate for an extended period and differentiate into mature cells both *in vitro* and *in vivo*. Methods to force the differentiation of human embryonic stem and induced pluripotent stem (iPS) cells into hepatic progenitor cells have been recently established. We demonstrated that the $CD13^{+}CD133^{+}$ fraction of human iPS-derived cells contained numerous hepatic progenitor-like cells. These analyses of hepatic stem/progenitor cells derived from somatic tissues and pluripotent stem cells will contribute to the development of new therapies for severe liver diseases.

Key words: hepatic stem/progenitor cells, liver regeneration, mesenchymal cells, pluripotent stem cells

INTRODUCTION

THE LIVER, THE largest organ in the body, regulates a multitude of metabolic functions. Parenchymal cells, also known as hepatocytes, express metabolic enzymes that are necessary for mature liver functions.[1] The non-parenchymal cells of the liver, such as stellate, sinusoidal endothelial, mesenchymal and Kupffer cells, regulate the functions of mature hepatocytes through cell–cell interactions. These metabolic functions are important for maintaining homeostasis. Therefore, liver damage induced by genetic mutations, viral infection and metabolic disorders may contribute to severe liver diseases such as liver fibrosis and hepatocellular carcinoma (HCC). Liver transplantation is a radical intervention to treat these diseases; however, this approach is limited in Japan due to a shortage of donor organs. Transplantation of hepatocytes or stem/progenitor cells in the liver may serve as an alternative treatment for severe liver diseases. Herein, we review work describing the role of stem and progenitor cell systems in liver regeneration and development. In addition, we discuss the application of liver stem/progenitor cells in future regenerative therapies.

Correspondence: Dr Akihide Kamiya, Laboratory of Stem Cell Therapy, Institute of Innovative Science and Technology, Tokai University, 143 Shimokasuya, Isehara, Kanagawa 259-1193, Japan. Email: kamiyaa@tokai-u.jp
Received 17 March 2014; revision 13 April 2014; accepted 24 April 2014.

LIVER REGENERATION

REGENERATION AFTER HEPATECTOMY or chemical-induced injury is an example of the remarkable abilities of the liver. Approximately 70% of the liver mass can be surgically removed by partial hepatectomy, and the remnants of the liver can expand and compensate its functions. Liver regeneration reportedly depends primarily on the proliferation of adult hepatocytes.[2] In the first step of liver regeneration, interleukin (IL)-6 is produced from non-parenchymal cells, priming mature hepatocytes for proliferation.[3]

Next, growth factors including hepatocyte growth factor (HGF) are induced and mature hepatocytes enter into the S-phase.[4,5] Subsequently, proliferation of non-parenchymal cells is induced and liver regeneration is completed.

During liver regeneration, hepatocytes also undergo hypertrophy. Hypertrophy was recently identified as an important process involved in regeneration induced by partial hepatectomy.[6] Recovery from 30% and 70% partial hepatectomy was shown to rely on different mechanisms. Hypertrophy of mature hepatocytes is sufficient for recovery from 30% hepatectomy. While hypertrophy is involved in the early phase of recovery from 70% partial hepatectomy, hepatocytes enter the cell cycle in the latter phase of regeneration. Therefore, the mechanisms involved in liver regeneration, hypertrophy and proliferation are regulated by the severity of liver injury.

In contrast to regeneration induced by acute liver damage, severe and chronic liver damage induces the defect of proliferation of mature hepatocytes.[7] Stem and progenitor cells in the adult liver are thought to be involved in regeneration induced by these chronic liver damage; however, the mechanisms underlying this process remain largely unknown.

STEM/PROGENITOR CELL SYSTEMS IN THE LIVER

Somatic stem cells and pluripotent stem cells

STEM CELLS, GENERALLY defined as clonogenic cells, exhibit properties of self-renewal, multipotency (producing progeny belonging two or more lineages) and long-term tissue repopulation after transplantation. Two types of stem cells exist, somatic and pluripotent stem cells. During development of several tissues, somatic stem cells give rise to non-self-renewing progenitors with restricted differentiation potential. Functionally mature cells are generated while a subpopulation of primitive stem cells is maintained. Thus, stem cells are involved in organ formation during developmental stages, and organ maintenance and repair in the adults. Pluripotent embryonic stem (ES) cells, derived from the inner cell mass of the blastocyst, give rise to tissues derived from the three primary germ layers: ectoderm, mesoderm and endoderm.[8,9] Induced pluripotent stem (iPS) cells, generated from somatic cells by simultaneously expressing Yamanaka factors (*Oct3/4*, *Klf4*, *Sox2* and *c-Myc*), have properties similar to those of ES cells.[10,11]

Stem/progenitor cell systems in the fetal liver

Two types of liver stem/progenitor cells are widely recognized. In contrast to adult liver stem/progenitor cells that are involved in regeneration, stem/progenitor cells in fetal liver are important for embryonic liver development. At the onset of liver development at approximately mouse embryonic day (E)9, hepatic progenitor cells (HPC) differentiate from foregut endoderm and expand to form the early fetal liver bud.[12,13] Characterization of HPC in fetal livers was recently advanced by the advent of a novel flow cytometry screening method.[14] Mouse fetal liver cells were dissociated and fractionated using specific cell-surface marker antibodies. Individual fractionated cells were sorted onto the wells of dishes and evaluated for their colony-forming ability and expression of hepatocytic and cholangiocytic markers (Fig. 1). Large colonies formed from single cells derived from E9.5–14.5 livers were positive for albumin and cytokeratin (CK)19, markers of hepatocytes and cholangiocytes, respectively. Mouse hepatic stem/progenitor cell-specific surface markers, such as DLK, LIV2, CD13, E-cadherin and CD133, were identified using this method (Table 1).[15–19]

Using this colony formation culture system, proliferation and differentiation of HPC in fetal livers were shown to be regulated by several transcription factors, including prospero-related homeobox 1 and its binding partner, liver receptor homolog 1, that cooperatively regulate development of HPC.[20] The transcription factor Sal-like protein 4 (SALL4) has been shown to regulate organogenesis, embryogenesis and maintenance of pluripotency. We found that SALL4 plays a crucial role in controlling the lineage commitment of HPC not only through inhibiting their differentiation into hepatocytes, but also by driving their differentiation into cholangiocytes.[21] In addition, our group and others reported that SALL4 is also important for stemness of liver cancers.[22–24] Cancers have a subpopulation of stem-like cells, or tumor-initiating cells, that are similar to somatic stem/progenitor cells. SALL4 is expressed in fetal liver stem/progenitor cells, but not normal adult hepatocytes. We demonstrated that SALL4 is also strongly expressed in human hepatocellular and cholangiocellular carcinomas. Elevated expression of SALL4 in tumors is associated with poor survival of HCC patients. Expression manipulation experiments showed that proliferation and stem cell marker expression in human HCC cells are regulated by SALL4 *in vitro* and *in vivo* (Fig. 2). Together, these results suggest that SALL4 is

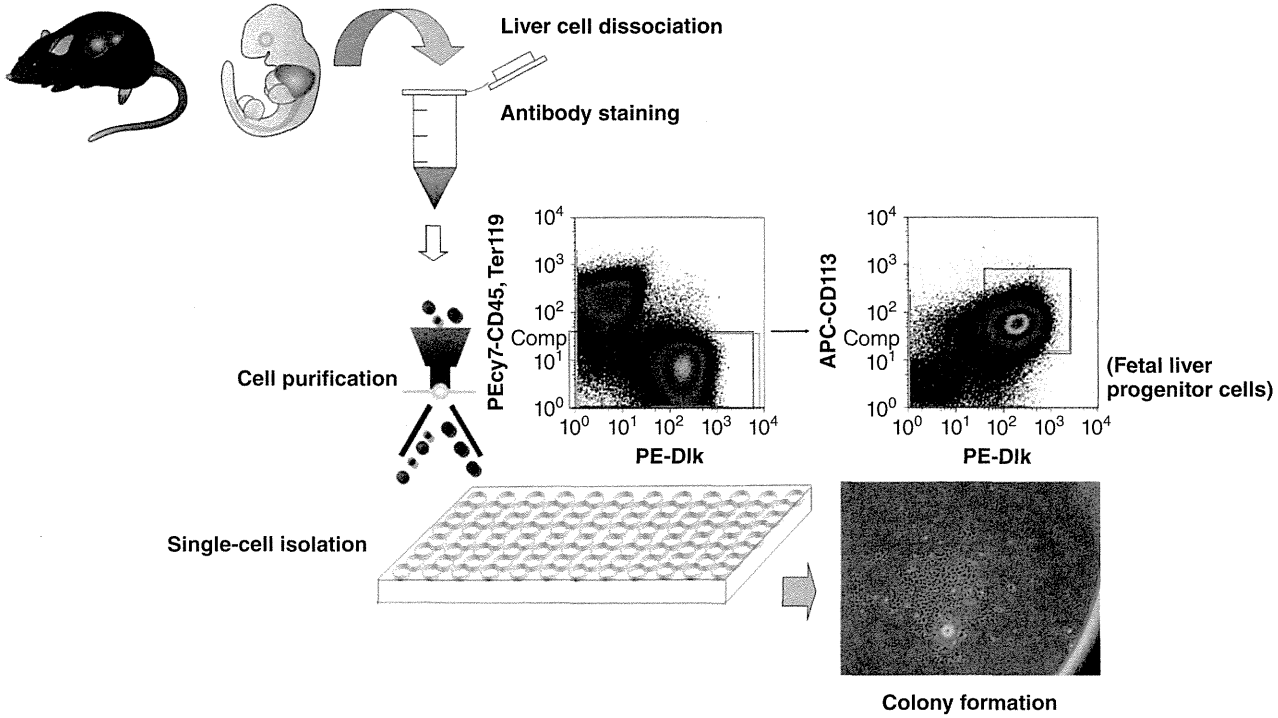

Figure 1 Colony formation assay using cells derived from fetal and adult livers. Liver cells were dissociated using collagenase and stained with stem/progenitor cell-specific antibodies. After the cells were purified using flow cytometry, individual cells were inoculated into the wells of collagen-coated culture dishes. Colonies derived from individual cells were analyzed.

a stem cell biomarker and a novel therapeutic target for liver cancers.

Regulation of fetal liver stem/progenitor cells by cell–cell interactions

During mid- to late fetal development (E11.5–16.5 in mice), hematopoietic stem cells originating from the aorta–gonad–mesonephros region migrate into the fetal liver.[25] Thus, the liver undergoes a dramatic change during development, transitioning from an embryonic hematopoietic tissue to a metabolic organ. We demonstrated that the interaction of HPC with hematopoietic cells is involved in their differentiation into mature hepatocytes.[26] HPC commence production of several metabolic enzymes involved in adult liver functions at mid- to late fetal stages. Oncostatin M (OSM), an IL-6 family cytokine, promotes hepatic maturation, as evidenced by the induction of metabolic enzymes and accumulation of glycogen. OSM is expressed in $CD45^+$ hematopoietic cells in mid-fetal livers, whereas OSM receptors are predominantly detected in hepatic cells, indicating that paracrine signaling from hematopoietic cells to HPC is important for fetal liver maturation.

In contrast to mid-fetal HPC, the *in vitro* characteristics of HPC at the onset of liver development (E9.5–10.5 in mice) are poorly elucidated, because no suitable culture system for these cells has been established. In early fetal liver development, endodermal and mesenchymal cells interact to promote liver bud growth. For example, the transcription factor H2.0-like homeobox protein, expressed in the septum transversum mesenchyme, is essential for early fetal liver development.[27] To mimic the interaction of hepatic and mesenchymal cells, we co-cultured mouse embryonic fibroblasts with HPC. Candidate HPC ($CD13^+Dlk^+$ cells) from early fetal livers that were clonally expanded using this novel culture system showed bipotency *in vitro*. Inhibition of Rho-associated protein kinase (Rock) or myosin II activity by using Y-27632 and blebbistatin, respectively, significantly enhanced the colony-forming activities of early fetal but not of mid-fetal HPC. These data suggested that purified HPC in early fetal livers have properties distinct from those in mid-fetal livers.[28]

Several mesenchymal cell types, including mesothelial, sub-mesothelial and transitional mesenchymal cells, have been identified in fetal livers.[29,30]

Table 1 Liver stem/progenitor cells in fetal and postnatal stages

Cell surface marker	Reference	Characteristics
1 Fetal stem/progenitor cells		
CD49f, c-Met	Suzuki *et al.*[14,49]	Clonal expansion of bipotent cells. *In vivo* transplantation.
Dlk	Tanimizu *et al.*[16]	Clonal expansion of bipotent cells. *In vivo* transplantation.
E-cadherin	Nitou *et al.*[19]	*In vitro* expansion.
Liv2	Watanabe *et al.*[15]	Expression in early and mid-fetal liver cells.
CD13	Kakinuma *et al.*[17]	Clonal expansion of bipotent cells. *In vivo* transplantation.
CD133	Kamiya *et al.*[18]	Clonal expansion of bipotent cells.
EpCAM	Schmelzer *et al.*[38]	Expansion of bipotent cells derived from human fetal livers. *In vivo* transplantation.
2 Postnatal stem/progenitor cells		
EpCAM	Okabe *et al.*[35]	Clonal expansion of bipotent cells derived from normal and injured livers.
EpCAM	Yovchev *et al.*[33]	Expression of oval cells in the injured rat livers. *In vivo* transplantation.
CD133	Suzuki *et al.*[34]	Clonal expansion of bipotent cells derived from injured livers. *In vivo* transplantation.
CD133	Rountree *et al.*[32]	Expansion and analyses cells derived from injured livers.
LGR5	Huch *et al.*[37]	*In vitro* organoid expansion. *In vivo* transplantation.
$CD13^+CD133^+$	Kamiya *et al.*[18]	Clonal expansion of bipotent cells derived from normal livers. *In vivo* transplantation.
$CD133^+MIC1\text{-}1C3^+$	Dorrell *et al.*[36]	Clonal expansion derived from normal and injured livers. *In vivo* transplantation
EpCAM	Schmelzer *et al.*[38]	Expansion of bipotent cells derived from human fetal livers. *In vivo* transplantation.

CD, cluster of differentiation; Dlk, delta-like 1 homolog; EpCAM, epithelial cell adhesion molecule; LGR, leucine-rich repeat-containing G-protein coupled receptor.

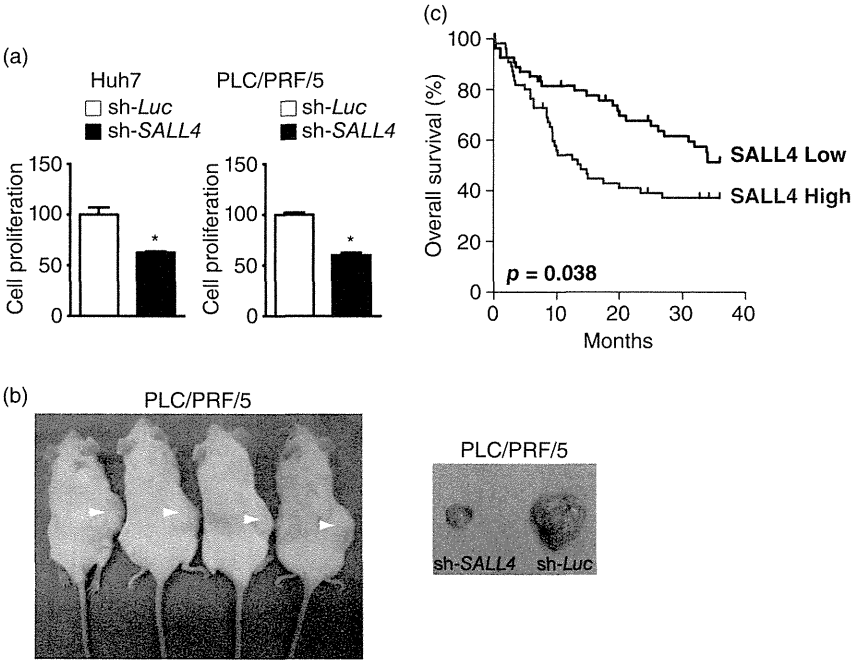

Figure 2 Sal-like protein 4 (SALL4) is a stem cell biomarker in liver cancers. (a) The effect of shRNA-mediated SALL4 downregulation on the proliferation of hepatocellular carcinoma (HCC) cell lines (Huh7 and PLC/PRF/5). sh-*Luc* was used as a negative control. (b) SALL4 downregulation affects xenograft tumor growth. (Left) Control PLC/PRF/5 and SALL4-knockdown cells were transplanted into recipient mice. Arrow heads show tumors derived from the control cells. (Right) Representative tumors derived from control and SALL4-knockdown cells. (c) Kaplan–Meier plot showing the survival of HCC patients expressing high and low levels of SALL4. (Reproduced from Oikawa *et al.* with permission).[22]

Platelet-derived growth factor receptor-α (PDGFRα) is a cell surface maker specifically expressed in fetal liver mesenchymal cells. We isolated PDGFRα$^+$ cells from fetal livers and co-cultured them with HPC using two culture systems: (i) a transwell culture system to analyze the effect of soluble factors on mesenchymal cells; and (ii) a direct co-culture system to analyze the effect of direct mesenchymal cell–HPC interactions.[31] Transwell co-culture significantly induced proliferation in HPC. These cells expressed minimal levels of albumin, a marker of hepatocyte differentiation. In contrast, expanded cells expressed significant levels of albumin when HPC were directly co-cultured, but proliferation of HPC was not increased. Therefore, the interactions between HPC and PDGFRα-expressing mesenchymal cells are important both for expansion of HPC and for induction of hepatic gene expression. Specifically, PDGFRα$^+$ cells had the potential to support HPC proliferation through secretion of soluble paracrine factors.

Stem/progenitor cell systems in the adult liver

A stem/progenitor cell system exists in normal adult livers and is thought to contribute to regeneration induced by severe liver injuries. During serious liver injury, such as that induced by retrorsine or 2-acetylaminofluorene treatment in combination with partial hepatectomy, the number of characteristic non-parenchymal oval cells increases in periportal regions. These cells express both cholangiocellular (*Ck7* and *19*) and hepatocellular marker genes (α-fetoprotein and albumin), and differentiate into both hepatocytic and cholangiocytic cells, suggesting that oval cells are candidate hepatic progenitors.[32–35]

However, the origin of oval cells is now under discussion. We recently purified CD13$^+$CD133$^+$ cells in non-injured postnatal livers and established an efficient single-cell culture system that involved the use of Rock inhibitor.[18] These CD13$^+$CD133$^+$ cell-derived colonies can expand for a prolonged period and differentiate into hepatocyte-like and cholangiocyte-like cells under appropriate culture conditions. These results show the presence of stem/progenitor cells in the CD13$^+$CD133$^+$ subpopulation of non-hematopoietic cells derived from non-injured postnatal livers. In addition, we speculate that oval cells may be transiently amplifying cells that originate from normal liver stem/progenitor cells (Fig. 3). Other postnatal cell surface markers were used for identification and purification of hepatic progenitor cells in normal and injured livers.[32–37] Hepatic progenitor cells were also identified in human livers. Schmelzer *et al.* showed that epithelial cell adhesion molecule positive cells in human fetal and adult livers can proliferate *in vitro* and expand after the transplantation into the injured mouse livers. Therefore, these

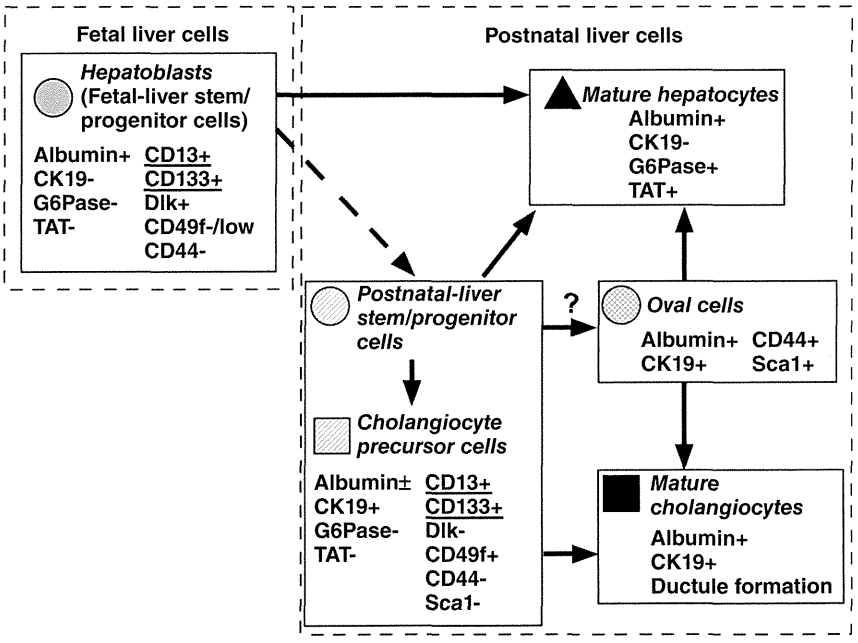

Figure 3 Embryonic and postnatal progenitor cell phenotypes during liver development. CD13 and CD133 are surface markers common to fetal-liver and postnatal-liver progenitor cells. CD, cluster of differentiation; CK, cytokeratin; Dlk, delta-like 1 homolog; G6Pase, glucose 6-phosphatase; Sca1, stem cell antigen 1; TAT, tyrosine aminotransferase. (Reproduced from Kamiya *et al.* with permission.)[18]